arXiv:1809.01344v1 [math.NA] 5 Sep 2018

Least Squares Finite Element Methods for Sea Ice Dynamics

Fleurianne Bertrand

5.09.2018

Abstract

A first-order system least squares formulation for the sea-ice dynamics is presented. In addition to the displacement field, the stress tensor is used as a variable. As finite element spaces, standard conforming piecewise polynomials for the displacement approximation are combined with Raviart-Thomas elements for the rows in the stress tensor. Computational results for a test problem illustrate the least-squares approach.

1 Introduction

Ice and snow covered surfaces reflect more than half of the solar radiation they are recieving and play therefore a major role in climate modelling. Each year, Antarctic sea ice extent reaches its maximum (17-20 million square kilometers) in September and its minimum (3-4 million square kilometers) in February. These important oscillations make the current predictive models of Antarctic sea ice require an accurate knowledge and understanding of the processes. Developing computational sea-ice modelling based on observed and measured data to study and predict the break-up and fracture evolution of sea-ice during the Antarctic spring was one of main scientific aims of the Winter 2017 cruise (Voyage 25) of the S.A. Agulhas II. This was funded by DST/NRF and took place from 28 June to 13 July 2017.

Sea ice is a complex material which is formed by the freezing of sea water. Since the ice stress is a source in the other equations of the climate models, its approximation plays an important role in the simulations of the ice. They can be computed from the velocity in a post-processing step, but the loss of accuracy due to the reconstruction step can lead to non-physical solutions. An alternative approach consists in the use of variational formulations involving the stress $\boldsymbol{\sigma} \in H(\text{div}, \Omega)$ as an independent variable. Appropriate finite element spaces based on a triangulation $\mathcal{T}$ are the $H(\text{div}, \Omega)$-conforming spaces, e.g. the Raviart-Thomas Space.

2 Problem Formulation

As most sea ice dynamic models currently used, our model is based on the viscous-plastic formulation introduced by Hibler [5]. There, sea ice is modeled by its velocity $\mathbf{u}$, the ice concentration A and the average ice height H over a domain Ω. The model consists in a momentum equation for the velocity $\mathbf{u}$ and the balance laws for ice concentration A and the average ice height H. Neglegting the thermodynamical effects,

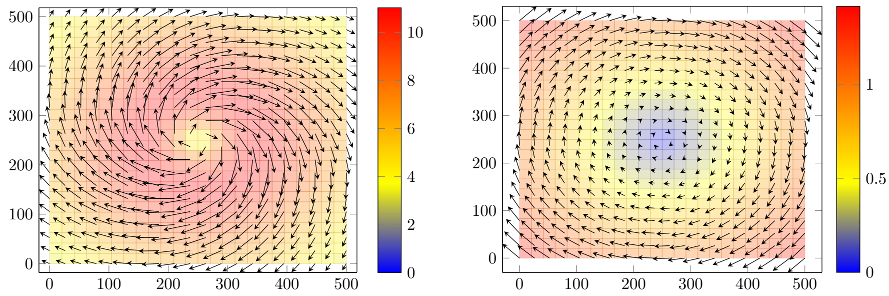

Figure 1: Wind field at $t = 0$ (left) and Ocean current (right)

i.e. the source terms in these balance laws, the model can be written as

$$
\begin{aligned}
\rho_{ice} H \frac{\partial \mathbf{u}}{\partial t} + \mathbf{F}(\mathbf{u}) - \operatorname{div} \boldsymbol{\sigma}(\mathbf{u}, A, H) = 0, \\
\frac{\partial A}{\partial t} + \operatorname{div}(\mathbf{u}A) = 0, \quad \frac{\partial H}{\partial t} + \operatorname{div}(\mathbf{u}H) = 0 \,,
\end{aligned} \tag{1}
$$

where the force term involving the ice, air and water densities ρ_{ice},ρ_a and ρ_o, the air and water drag coefficients C_a and C_o, the coriolis parameter f_c, the radial unit vector $\mathbf{e}_r$ and the velocity fields $\mathbf{v}_o$ and $\mathbf{v}_a$ of ocean and atmospheric flow is given by

$$
\mathbf{F}(\mathbf{v}) = f_c \mathbf{e}_r \times (\mathbf{v} - \mathbf{v}_o) - \underbrace{\rho_a C_a \|\mathbf{v}_a\|_2 \mathbf{v}_a}_{=:\boldsymbol{\tau}_a} - \underbrace{\rho_o C_o \|\mathbf{v}_o - \mathbf{v}\|_2 (\mathbf{v}_o - \mathbf{v})}_{=:\boldsymbol{\tau}_o(\mathbf{v})} \tag{2}
$$

and the stress-strain relation involving the ice strength parameter $P^\star$ and the ice concentration parameter C is given by

$$
\begin{aligned}
\boldsymbol{\sigma} = \frac{P}{2} \left(\frac{\operatorname{dev} \boldsymbol{\varepsilon}(\mathbf{u}) + 2\operatorname{tr} \boldsymbol{\varepsilon}(\mathbf{u}) \mathbf{I}}{\Delta(\mathbf{u})} - \mathbf{I} \right) \quad \text{with } P = P^\star H e^{-C(1-A)} \\
\text{and } \; \Delta(\mathbf{u}) = \sqrt{\operatorname{dev} \boldsymbol{\varepsilon}(\mathbf{u}) : \operatorname{dev} \boldsymbol{\varepsilon}(\mathbf{u}) + 4 \operatorname{tr}(\boldsymbol{\varepsilon}(\mathbf{u}))^2 + \Delta_{min}^2}
\end{aligned} \tag{3}
$$

where $\Delta_{min} = 2 \cdot 10^{-9}\ s^{-1}$ is a limitation for $\Delta(\mathbf{u})$. In [7], the authors propose a variational formulation where $(\mathbf{u}, \mathbf{p})$ with $\mathbf{p} = (A, H)$ is sought in $\left(H_0^1(\Omega)\right)^2 \times \left(L^2(\Omega)\right)^2$ such that

$$
\begin{aligned}
\left(\rho_{ice} H \frac{\partial \mathbf{u}}{\partial t}, \mathbf{v} \right) + (\mathbf{F}(\mathbf{u}), \mathbf{v}) + (\boldsymbol{\sigma}(\mathbf{u}, H, A), \nabla \mathbf{v}) = 0, \\
\left(\frac{\partial \mathbf{p}}{\partial t} + \nabla \mathbf{p} \cdot \mathbf{u} + \operatorname{div}(\mathbf{u}) \mathbf{p}, \mathbf{q} \right) = 0
\end{aligned} \tag{4}
$$

holds for all $(\mathbf{v}, \mathbf{q}) \in \left(H_0^1(\Omega)\right)^2 \times \left(L^2(\Omega)\right)^2$. The constraints $H \geq 0$ and $A \in [0, 1]$ are embedded in the trial-spaces and are realized by a projection of the solution.

3 A Least-Squares Method

The Least-Squares Mehtod (see [2]) consists in minimizing the L^2-residuals in the partial differential equations. Therefore, we insert define a new variable $\boldsymbol{\sigma}$ for the stress and consider the stress-strain relationship (3) as and additional equation in order to obtain the following first order system for $(\boldsymbol{\sigma}, \mathbf{u}, A, H)$:

$$
\begin{aligned}
\rho_{ice} H \frac{\partial \mathbf{u}}{\partial t} + \mathbf{F}(\mathbf{u}) - \operatorname{div} \boldsymbol{\sigma} = 0 \qquad & \frac{\partial A}{\partial t} + \operatorname{div}(\mathbf{v}A) = 0 \\
\frac{P(A,H)}{2}\left(\frac{\operatorname{dev} \boldsymbol{\varepsilon}(\mathbf{u})}{\Delta(\mathbf{u})} + \frac{2\operatorname{tr} \boldsymbol{\varepsilon}(\mathbf{u})}{\Delta(\mathbf{u})}\mathbf{I} - \mathbf{I}\right) = \boldsymbol{\sigma} \qquad & \frac{\partial H}{\partial t} + \operatorname{div}(\mathbf{v}H) = 0
\end{aligned}
$$

The least-squares functionals then reads

$$
\mathcal{F}(\boldsymbol{\sigma}, \mathbf{u}, H) = \mathcal{F}_m(\boldsymbol{\sigma}, \mathbf{u}, A, H) + \mathcal{F}_c(\boldsymbol{\sigma}, \mathbf{u}, A, H) + \mathcal{F}_e(\boldsymbol{\sigma}, \mathbf{u}, A, H) \tag{5}
$$

with

$$
\begin{aligned}
\mathcal{F}_m(\boldsymbol{\sigma}, \mathbf{u}, A, H) &= \left\| \rho_{ice} H \frac{\partial \mathbf{u}}{\partial t} + \mathbf{F}(\mathbf{u}) - \operatorname{div} \boldsymbol{\sigma} \right\|_0^2, \\
\mathcal{F}_e(\boldsymbol{\sigma}, \mathbf{u}, A, H) &= \left\| \frac{\partial H}{\partial t} + \operatorname{div}(\mathbf{u}H) \right\|_0^2 + \left\| \frac{\partial A}{\partial t} + \operatorname{div}(\mathbf{u}A) \right\|_0^2, \\
\mathcal{F}_c(\boldsymbol{\sigma}, \mathbf{u}, A, H) &= \left\| \boldsymbol{\sigma} - \frac{P(A,H)}{2}\left(\frac{\operatorname{dev} \boldsymbol{\varepsilon}(\mathbf{u})}{\Delta(\mathbf{u})} + \frac{\operatorname{tr} \boldsymbol{\varepsilon}(\mathbf{u})}{\Delta(\mathbf{u})}\mathbf{I} - \mathbf{I}\right) \right\|_0^2 .
\end{aligned}
$$

The time discretization can be realised using a θ-scheme and decoupling the advection equations from the rest of the system such that for each time step $n+1$, the linear functional

$$
\begin{aligned}
\mathcal{G}^{n+1}(A^{n+1}, H^{n+1}; \mathbf{u}^n, H^n, A^n) = &\left\| \frac{H^{n+1} - H^n}{t^\Delta} + \operatorname{div}(\mathbf{u}^n H^{n+1}) \right\|_0^2 \\
&+ \left\| \frac{A^{n+1} - A^n}{t^\Delta} + \operatorname{div}(\mathbf{u}^n A^{n+1}) \right\|_0^2
\end{aligned} \tag{6}
$$

is first minimized over all $(A^{n+1}, H^{n+1}) \in \left(L^2(\Omega)\right)^2$, and then the functional

$$
\begin{aligned}
&\mathcal{F}^{n+1}(\boldsymbol{\sigma}^{n+1}, \mathbf{u}^{n+1}; \boldsymbol{\sigma}^n, \mathbf{u}^n, A^{n+1}, H^{n+1}) \\
&\qquad = \left\| \rho_{ice} H^{n+1} \frac{\mathbf{u}^{n+1} - u^n}{t^\Delta} + \mathbf{F}(\mathbf{u}^{n+\theta}) - \operatorname{div} \boldsymbol{\sigma}^{n+\theta} \right\|_0^2 \\
&\qquad + \mathcal{F}_c(\boldsymbol{\sigma}^{n+1}, \mathbf{u}^{n+1}; A^{n+1}, H^{n+1})
\end{aligned} \tag{7}
$$

with the time discretized variables

$$
\mathbf{u}^{n+\theta} = \theta \mathbf{u}^{n+1} + (1-\theta)\mathbf{u}^n
$$

and

$$
\boldsymbol{\sigma}^{n+\theta} = \theta \boldsymbol{\sigma}^{n+1} + (1-\theta)\boldsymbol{\sigma}^n ,
$$

is minimized over all $(\boldsymbol{\sigma}^{n+1}, \mathbf{u}^{n+1}) \in (H_{\text{div}}(\Omega))^2 \times \left(H^1_{\Gamma_D}(\Omega)\right)^2$. For the spacial discretization, a conforming subspace $\mathbf{W}_h$ of $(H_{\text{div}}(\Omega))^2 \times \left(H^1_{\Gamma_D}(\Omega)\right)^2 \times \left(L^2(\Omega)\right)^2$. Therefore, a triangulation $\mathcal{T}_h$ of the domain Ω is considered. In this work, we choose $\mathbf{W}_h = (RT_1^2(\mathcal{T}_h) \times \mathcal{P}_2^2(\mathcal{T}_h)) \times \mathcal{P}_1^2(\mathcal{T}_h))$ in order to have appropriate convergence properties.

For the minimization of the nonlinear Functional $\mathcal{F}^{n+1}$ in each time step, the Least-Squares Functional is linearized around a given approximation $(\boldsymbol{\sigma}^k, \mathbf{u}^k, A^k, H^k)$ and the minimization is then carried out iteratively solving a sequence of linearized least squares problems. Additionaly the Least-Squares Functional is minimized subejct to the linear inequality constraints $A \in [0,1]$ and $H \geq 0$, that leads to a constraint optimization problem that we solved with an active set strategy. Since the variables A and H are now decoupled from $\mathbf{u}$ and $\boldsymbol{\sigma}$, we can define the stress-strain relation ship by

$$\mathcal{C}(\mathbf{u}; A, H) := \boldsymbol{\sigma}(\mathbf{u}; A, H) = \frac{P(A,H)}{2}\left(\frac{\text{dev }\boldsymbol{\varepsilon}(\mathbf{u}) + 2\text{tr }\boldsymbol{\varepsilon}(\mathbf{u})\mathbf{I}}{\Delta(\mathbf{u})} - \mathbf{I}\right) \tag{8}$$

The Gateaux derivative of $\mathcal{C}(\mathbf{u}; A, H)$ in direction $\mathbf{v}$ is denoted by $\mathcal{C}(\mathbf{u}; A, H)[\mathbf{v}]$ and given by

$$\mathcal{J}_{\mathcal{C}}(\mathbf{u}; A, H)[\mathbf{v}] = \frac{P(A,H)}{2}\left(\frac{\text{dev }\boldsymbol{\varepsilon}(\mathbf{v}) + 2\text{tr }\boldsymbol{\varepsilon}(\mathbf{v})\mathbf{I}}{\Delta(\mathbf{u})} + \mathcal{J}_{\Delta^{-1}}(\mathbf{u})[\mathbf{v}]\,(\text{dev }\boldsymbol{\varepsilon}(\mathbf{u}) + 2\text{tr }\boldsymbol{\varepsilon}(\mathbf{u})\mathbf{I})\right) \tag{9}$$

with $\mathcal{J}_{\Delta^{-1}}(\mathbf{u})[\mathbf{v}] = -\Delta(\mathbf{u})^{-3}\,(\text{dev }\boldsymbol{\varepsilon}(\mathbf{u}) : \text{dev }\boldsymbol{\varepsilon}(\mathbf{v}) + 4\text{tr}(\boldsymbol{\varepsilon}(\mathbf{u}))\text{tr}(\boldsymbol{\varepsilon}(\mathbf{v})))$.

The first variation of the minimization of $\mathcal{F}^{n+1}$ is then given by

$$\begin{aligned}
\mathcal{B}(\boldsymbol{\sigma}^{n+1}, &\mathbf{u}^{n+1}; \boldsymbol{\tau}, \mathbf{v}; \boldsymbol{\sigma}^n, \mathbf{u}^n, A^{n+1}, H^{n+1}) = \left.\frac{\partial \mathcal{F}^{n+1}(\boldsymbol{\sigma}^{n+1} + \tau\boldsymbol{\tau}, \mathbf{u}^{n+1} + \tau\mathbf{v}; \boldsymbol{\sigma}^n, \mathbf{u}^n, A^n, H^n)}{\partial\tau}\right|_{\tau=0} \\
&= \frac{\partial}{\partial\tau}\left(\boldsymbol{\sigma}^{n+1} + \tau\boldsymbol{\tau} - \mathcal{C}(\mathbf{u}^{n+1} + \tau\mathbf{v}; A^{n+1}, H^{n+1}), \boldsymbol{\sigma}^{n+1} + \tau\boldsymbol{\tau} - \mathcal{C}(\mathbf{u}^{n+1} + \tau\mathbf{v}; A^{n+1}, H^{n+1})\right)\Big|_{\tau=0} \\
&\quad + 2\left(\rho_{ice}H^{n+1}\frac{\mathbf{u}^{n+1} - u^n}{t^\Delta} - \text{div}(\theta\boldsymbol{\sigma}^{n+1} + (1-\theta)\boldsymbol{\sigma}^n), \rho_{ice}H^{n+1}\frac{\theta\mathbf{v}}{t^\Delta} - \text{div}(\theta\boldsymbol{\tau})\right) \\
&\quad + \frac{\partial}{\partial\tau}\left(\mathbf{F}(\theta\mathbf{u}^{n+1} + \theta\tau\mathbf{v} + (1-\theta)\mathbf{u}^n), \mathbf{F}(\theta\mathbf{u}^{n+1} + \theta\tau\mathbf{v} + (1-\theta)\mathbf{u}^n)\right)\Big|_{\tau=0} \\
&\quad +2\,\frac{\partial}{\partial\tau}\left(\rho_{ice}H^{n+1}\frac{\mathbf{u}^{n+1} + \tau\mathbf{v} - u^n}{t^\Delta} - \text{div}(\theta\boldsymbol{\sigma}^{n+1} + \theta\tau\boldsymbol{\tau} + (1-\theta)\boldsymbol{\sigma}^n), \mathbf{F}(\theta\mathbf{u}^{n+1} + \theta\tau\mathbf{v} + (1-\theta)\mathbf{u}^n)\right)\Big|_{\tau=0} \\
&= 2\left(\boldsymbol{\sigma}^{n+1} - \mathcal{C}(\mathbf{u}^{n+1}; A^{n+1}, H^{n+1}), \boldsymbol{\tau} - J_{\mathcal{C}}(\mathbf{u}^{n+1}; A^{n+1}, H^{n+1})[\mathbf{v}]\right) \\
&\quad + 2\left(\rho_{ice}H^{n+1}\frac{\mathbf{u}^{n+1} - u^n}{t^\Delta} + \mathbf{F}(\mathbf{u}^{n+\theta}) - \text{div }\boldsymbol{\sigma}^{n+\theta}, \rho_{ice}H^{n+1}\frac{\mathbf{v}}{t^\Delta} + J_{\mathbf{F}}(\mathbf{u}^{n+\theta})[\theta\mathbf{v}] - \theta\text{div }\boldsymbol{\tau}\right).
\end{aligned}$$

Setting this first variation to zero leads to a necessary condition such that the Gauß-Newton Methods in each time step consits in setting iterativly $(\boldsymbol{\sigma}^{n+1,k+1}, \mathbf{u}^{n+1,k+1}) = (\boldsymbol{\sigma}^{n+1,k}, \mathbf{u}^{n+1,k}) + (\delta\boldsymbol{\sigma}, \delta\mathbf{u})$ where $(\delta\boldsymbol{\sigma}, \delta\mathbf{u}) \in (RT_0^2(\mathcal{T}_h) \times \mathcal{P}_1^2(\mathcal{T}_h))$ is the solution of

$$\begin{aligned}
\mathcal{B}(\boldsymbol{\sigma}^{n+1,k}, \mathbf{u}^{n+1,k}; \boldsymbol{\tau}, \mathbf{v}; \boldsymbol{\sigma}^n, \mathbf{u}^n, A^{n+1}, H^{n+1}) &= \left(\delta\boldsymbol{\sigma} - J_{\mathcal{C}}(\mathbf{u}^{n+1,k}; A^{n+1}, H^{n+1})[\delta\mathbf{u}], \boldsymbol{\tau} - J_{\mathcal{C}}(\mathbf{u}^{n+1,k}; A^{n+1}, H^{n+1})[\mathbf{v}]\right) \\
+ \Big(\rho_{ice}H^{n+1}\frac{\delta\mathbf{u}}{t^\Delta} + J_{\mathbf{F}}(\theta\mathbf{u}^{n+1,k} + (1-\theta)\mathbf{u}^n)[\theta\delta\mathbf{u}] - \theta\text{div }\delta\boldsymbol{\sigma}&, \rho_{ice}H^{n+1}\frac{\mathbf{v}}{t^\Delta} + J_{\mathbf{F}}(\theta\mathbf{u}^{n+1,k} + (1-\theta)\mathbf{u}^n)[\theta\mathbf{v}] - \theta\text{div }\boldsymbol{\tau}\Big)
\end{aligned}$$

for all $(\boldsymbol{\tau}, \boldsymbol{\sigma}) \in (RT_0^2(\mathcal{T}_h) \times \mathcal{P}_1^2(\mathcal{T}_h))$.

4 Test Case

In order to investigate the approximation properties of the Least-Squares method, we consider the same test case as in [7], involving a quadratic domain (see also [6]) and

Parameter	Value
maximal ocean velocity v_o^m	$0.01\ \mathrm{ms}^-1$
maximal ocean velocity v_a^m	$15\ \mathrm{ms}^-1$
sea ice density ρ_{ice}	$900\ \mathrm{kg\ m}^-3$
air density ρ_a	$1.3\ \mathrm{kg\ m}^-3$
water density ρ_o	$1026\ \mathrm{kg\ m}^-3$
air drag coefficient C_a	$1.2 \cdot 10^{-3}$
water C_o	$5.5 \cdot 10^{-3}$
coriolis parameter f_c	$1.46 \cdot 10^{-4}\ \mathrm{s}^-1$
ice strength parameter $P^\star$	$27.5 \cdot 10^3\ \mathrm{Nm}^-2$
ice concentration parameter C	20

Figure 2: Parameter used in the simulation

simulating the sea ice dynamics for $T = 8$ days. Since the Least-Squares Method approximates all the residuals of the partial differential equation simultaneously, we scale the domain to the unit square $\Omega = [0,1]^2$. Since the wind field is a cyclone from the midpoint of the computational domain to the edge followed by an anticyclone diagonally passing from the edge to the midpoint, we define the time $t^m = t - 4$ measured in days with respect to the time when the wind forcing alternates from cyclonic to anticyclonic. Further, let $\tilde{\mathbf{x}}(t) = \mathbf{x} - \mathbf{x}^m(t)$ denote the position with respect to the center of the cyclone $\mathbf{x}^m(t) = x^m(t)(\mathbf{e}_1 + \mathbf{e}_2)$ with $x^m(t) = 0.1(9 - |t^m|)$. Then, the prescribed wind field is given by

$$\mathbf{v}_a = 10 v_a^m \left(1 - \frac{2}{e^{t^m} e^{8-|t^m|} + 1}\right) e^{-\frac{\|\tilde{\mathbf{x}}(t)\|_2}{10}} \mathbf{R}\left(\frac{17}{40}\pi + \frac{t^m}{40|t^m|}\pi\right) \tilde{\mathbf{x}} \tag{10}$$

$$\text{with } \mathbf{R}(\vartheta) = \begin{pmatrix} \cos\vartheta & -\sin\vartheta \\ \sin\vartheta & \cos\vartheta \end{pmatrix}, \tag{11}$$

and a maximal wind velocity v_a^m, while the circular steady ocean current is

$$\mathbf{v}_o = v_o^m \begin{pmatrix} 2y - 1 \\ 1 - 2x \end{pmatrix} \tag{12}$$

with a maximal ocean velocity v_o^m. Finally, the initial conditions are given by zero velocity, constant ice concentration $A = 1$ and $H^0(x,y) = 0.3 + 0.005(\sin(250x) + \sin(250y))$. All simulations are executed with Fenics, using the inherent Newton solver. The velocity results at $t = 2,4,6,8$ days are shown in the figure 3. Further intervestigations are needed, in particular regarding the ellipticity of the Least-Squares Functional, the possibility of considering domain with curved boundaries (see [1]) and the relation to others standard or mixed methods (as in [4]).

References

[1] F. Bertrand, S. Münzenmaier, and G. Starke *First-order System Least Squares on Curved Boundaries: Higher-order Raviart–Thomas Elements*. SIAM J. Numer. Anal. (2014) 52, 3165-3180.

[2] P. BOCHEV AND M. GUNZBURGER, *Least-Squares Finite Element Methods*, Springer, New York, 2009.

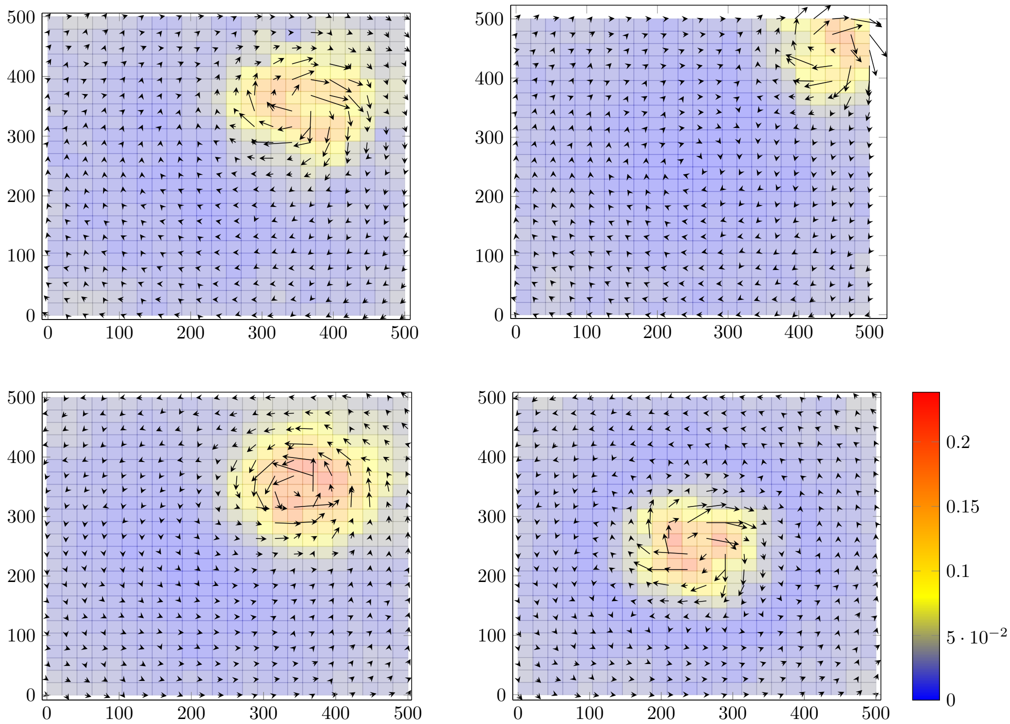

Figure 3: Sea-ice velocity at $t = 2, 4, 6, 8$.

[3] D. BOFFI, F. BREZZI, AND M. FORTIN, *Mixed Finite Element Methods and Applications*, Springer, Heidelberg, 2013.

[4] J. Brandts, Y. Chen and J. Yang *A note on least-squares mixed finite elements in relation to standard and mixed finite elements*. IMA J. Numer. Anal. (2006) 26: 779-789.

[5] W.D. Hibler *A dynamic thermodynamic sea ice model*. J. Phys. Oceanogr (1979) 566 9(4):815-846.

[6] E.C. Hunke *Viscous-plastic sea ice dynamics with the EVP model: linearization isues*. J. Comp. Phys. (2001) 170:18-38.

[7] C. Mehlmann und T. Richter, *A modified global Newton solver for viscous-plastic sea ice models*, Ocean Modeling, Vol. 116, p.96:107, 2017.